1 **Electron transport chain biogenesis activated by a JNK-insulin-Myc relay primes**

2 **mitochondrial inheritance in *Drosophila***

3

4 Zong-Heng Wang[1], Yi Liu[1], Vijender Chaitankar[1], Mehdi Pirooznia[1], and Hong Xu[1,*]

5

6 [1]National Heart, Lung, and Blood Institute, National Institutes of Health, Bethesda, MD

7 20892, USA

8 [*]Correspondence: Hong.Xu@nih.gov

Wang et al., 2019

SUMMARY

Oogenesis features an enormous increase in mitochondrial mass and mtDNA copy number, which are required to furnish mature eggs with adequate mitochondria and to curb the transmission of deleterious mtDNA variants. Quiescent in dividing germ cells, mtDNA replication initiates upon oocyte determination in the *Drosophila* ovary, which necessitates active mitochondrial respiration. However, the underlying mechanism for this dynamic regulation remains unclear. Here, we show that an feedforward insulin-Myc loop promotes mitochondrial respiration and biogenesis by boosting the expression of electron transport chain subunits and factors essential for mtDNA replication and expression, and mitochondrial protein import. We further reveal that transient activation of JNK enhances the expression of insulin receptor and initiates the insulin-Myc signaling loop. Importantly, this signaling relay ensures sufficient mtDNA in eggs and limits the transmission of a deleterious mtDNA mutation. Our study demonstrates cellular mechanisms that couple mitochondrial biogenesis and inheritance with oocyte development.

INTRODUCTION

Mitochondria host a number of biosynthetic pathways and produce most cellular ATP through oxidative phosphorylation carried out by the electron transport chain complexes (ETC) on mitochondrial inner membrane. While the majority of mitochondrial proteins are encoded on the nuclear genome, synthesized in cytoplasm, and imported to mitochondria, a subset of core ETC components are encoded on the mitochondrial genome (mtDNA) and synthesized inside the mitochondrial matrix. Thus, mitochondria biogenesis and ETC activity in particular, rely on the coordinated expression of both nuclear encoded mitochondrial genes and mtDNA (Falkenberg et al., 2007). To meet the diverse energy demands and metabolic programs of the cell, the abundance of mitochondria and their activity differ in a variety of tissues and developmental processes. Mitochondria are transmitted exclusively through maternal lineage in most metazoans (Wallace, 2008), which demands complex regulations on mitochondrial biogenesis and ETC activity during oogenesis. Animal oocytes are hundreds of times larger than their progenitors (Picton et al., 1998). Accompanying this tremendous cell growth during oogenesis, mitochondria undergo prodigious biogenesis and mtDNA copy number increases over thousands of folds (Stewart et al., 2008). The massive amount of mitochondria in the mature oocyte is necessary to power the early embryonic development, as inadequate mitochondrial contents often lead to embryonic lethality (May-Panloup et al., 2007). However, the mechanism by which the germline couples mitochondrial biogenesis to oocyte development remains elusive.

In addition to furnishing mature oocytes with sufficient amount of mitochondria, oogenesis is also tasked with limiting the transmission of harmful mtDNA mutations. Mitochondrial genome is prone to accumulate mutations due to its close vicinity to the highly-mutagenic free radicals in the mitochondrial matrix and a lack of effective repair mechanisms (Pesole et al., 1999). Yet, harmful mtDNA mutations are rare in populations (Stewart and Larsson, 2014), underscoring the presence of efficient mechanisms to limit their transmission through the female germline. We previously reported that mtDNA replication depends on active respiration in the *Drosophila* ovary (Hill et al., 2014). Healthy mitochondria with wild type genome propagate more vigorously than defective ones afflicted with harmful mutations, which thereby curbs the

56 transmission of deleterious mtDNA mutations into the next generation (Zhang et al.,
57 2019). Therefore, active ETC appears to be a stress test for mtDNA functionality, and is
58 essential for mtDNA selective inheritance. Nonetheless, how the activity of ETC is
59 regulated during oogenesis is not well understood.

60   Insulin signaling (IIS), an evolutionary conserved pathway that controls cell
61 growth and proliferation (Oldham and Hafen, 2003), has also been shown to regulate
62 ETC biogenesis and ATP production in human skeletal muscles (Stump et al., 2003). In
63 the *Drosophila* ovary, IIS promotes the growth of follicles from early to middle stages of
64 oogenesis (LaFever and Drummond-Barbosa, 2005). Prior to the nurse cell dumping,
65 IIS activity is decreased, which relieves the inhibition on GSK3, and thereby shut down
66 mitochondrial respiration (Sieber et al., 2016). However, oogenesis begins with germline
67 stem cells (GSCs) that are considered not to obtain ATP from respiration (Kai et al.,
68 2005). We predicted there has to be developmental cues to activate mitochondrial
69 respiration in the late germarium stage when mtDNA replication commences. IIS
70 represents a logical candidate to modulate this metabolic transition in early oogenesis.
71 Nonetheless, it remains to be explored how IIS is dynamically regulated during
72 oogenesis and whether it is indeed involved in the aforementioned regulation.
73 Furthermore, little is known regarding how IIS modulates ETC activity and mtDNA
74 biogenesis in general.

75   In this study, we find that mitochondrial respiration is quiescent in GSCs and
76 dividing cysts, but markedly up-regulated in the late germarium, the same spatial-
77 temporal pattern as mtDNA replication. We uncovered a feedforward loop between IIS
78 and Myc protein which orchestrates the transcriptional activation of respiration and
79 mtDNA replication. Furthermore, transient JNK activity boosts insulin receptor (InR)
80 transcription to enhance the IIS-Myc loop. Our work uncovers how developmental
81 programs couple mitochondrial biogenesis with cell growth and its impact on
82 mitochondria inheritance.

83

RESULTS:

Coordinated transcription regulations on both nuclear and mitochondrial genome control ETC biogenesis

mtDNA replication is significantly increased in the post-mitotic germ cells in late germarium and relies on mitochondrial inner membrane potential (Ψ_m) and ETC activity (Hill et al., 2014). We therefore hypothesized that mitochondrial respiration might be developmentally regulated in a spatial-temporal pattern similar to that of mtDNA replication. To test this idea, we monitored Ψ_m, which is an indicator of mitochondrial respiration, in the developing germ cells. We found that Ψ_m, measured as the ratio of TMRM (an indicator for membrane potential) to MitoTracker Green (an indicator for mitochondrial mass) (Zhang et al., 2019), was markedly higher in region 2B than the earlier stages in the germarium (Fig 1A), indicating that respiration is activated in the 16-cell cysts, concomitantly with the onset of mtDNA replication. Consistently, ETC activity, indicated by a dual SDH (succinate dehydrogenase)/COX (cytochrome C oxidase) colorimetric assay (Ross, 2011), was much higher in region 2B than the earlier germarium stages and remained high until stage 10 egg chamber (Fig 1B and S1A). These results suggest that ETC activity is up-regulated in the late germarium stages.

We next asked whether the dynamic pattern of ETC activity in the germarium reflected the expression of ETC subunits. Except for complex II (SDH) that are encoded on nuclear genome only, all other ETC genes are encoded by both nuclear and mitochondrial genomes. Thus, we performed fluorescence *in situ* hybridization (FISH) with RNA probes specific to mRNAs of either nuDNA- or mtDNA-encoded ETC subunits in ovaries. Both COXIV (nuclear-encoded) and COXIII (mtDNA-encoded) transcripts exhibited low expression in earlier regions, but increased 4 to 6 folds in region 2B, recapitulating the pattern of ETC activity (Fig 1C and 1D). The same pattern was observed for Cyt-C1 (nuclear-encoded) and Cyt-B (mtDNA-encoded) (Fig. S1B). These results confirm that the increased ETC activity detected with our COX/SDH colorimetric assay indeed reflects an increase of ETC genes expression at region 2B germarium. Taken together, these data suggest that the activation of respiration at stage 2B relies on the coordinated transcription of nuDNA- or mtDNA-encoded genes.

A candidate RNAi screen for upstream regulators of ETC biogenesis

To uncover the upstream developmental cues that initiate ETC gene transcription in the late germarium, we screened a collection of 132 RNAi lines directed at major developmental signaling and factors involved in cellular metabolism and mitochondrial functions (Basson, 2012; Claveria and Torres, 2016; Desvergne et al., 2006; Perrimon et al., 2012). We expressed dsRNAs in the germ cells using a *nanos*-Gal4 (*nos*-Gla4) driver and applied the COX/SDH assay as an indirect measure of ETC abundance (Table S1). We also included a few RNAi lines directed at COX components or genes essential for mitochondrial biogenesis as positive controls. As expected, knock down of these genes consistently impaired ETC activity (Fig 2A). Overall, 6 RNAi lines from the list caused germline degeneration and 12 lines led to reduced ETC activity without causing the loss of germline or defects in development (Fig S2A). Among these 12 lines are components of the IIS/TORC1 signaling, the JNK pathway, cell adhesion molecules, translation regulators and one transcription factor. Notably, all hits impaired activities of both COX and SDH, except for *coxV* RNAi that disrupted COX activity only, indicating that the recovered genes are required for the expression of both nuclear and mitochondrial genes.

Myc controls ETC biogenesis and mtDNA replication

The transcription factor Myc emerged as one of the strongest hits from our screen. Additionally, we found that Myc's expression pattern, monitored with a Myc-GFP fusion protein (Greer et al., 2013), mirrored the pattern of ETC activity in the ovary: low in the early stages, but elevated in germarium region 2B and remaining high until mid-stage egg chambers (Fig 2B and S2B). These observations spurred us to explore the potential roles of Myc in the activation of ETC genes expression at stage 2B. To confirm the result of the Myc RNAi experiment, we utilized a hypomorphic Myc allele, myc^{P0}, which has reduced level of *myc* mRNA, but progresses through early oogenesis (Johnston et al., 1999; Quinn et al., 2004). Consistent with the RNAi result, the myc^{P0} mutation led to a reduction in ETC activity and mtDNA replication (Fig 2C-2F). Next, to test whether Myc is sufficient for ETC activity induction, we utilized *bam-Gal4* to over-express myc ORF in the dividing cyst in region 2A that normally have low levels of both

146   ETC activity and Myc protein. Over-expression of *myc* in this region ectopically

147   enhanced ETC activity (Fig 2C and 2D). Thus, Myc is both necessary and sufficient to

148   stimulate mitochondrial respiration in the ovary.

149   To gain insight into how Myc regulates mitochondrial biogenesis, we compared

150   the transcriptomes of wt and myc^{P0} mutant ovaries (Table S2). RNA sequencing

151   (RNAseq) showed that nearly one third of detected transcripts were reduced in myc^{P0}

152   mutant compared to wt (fold change>3.0, FDR<0.05%) (Fig 2G), consistent with the

153   notion of Myc as a general transcription activator (Orian et al., 2003). Importantly,

154   nuclear-encoded mitochondrial genes were enriched among the down-regulated genes.

155   About 52% of the total mitochondrial genes, and 75% of ETC genes and factors for

156   mtDNA replication and expression were decreased. Myc directly regulates the

157   expression of its targets by binding to a short sequence, CACGTG (E-box) in the

158   regulatory region. Interestingly, 406 out of 477 down-regulated mitochondrial genes

159   have predicted Myc binding sites in their regulatory regions, further substantiating a role

160   of Myc in promoting mitochondrial biogenesis *via* boosting the transcription of

161   mitochondrial genes (Fig 2H). Additionally, 48 transcriptional factors, 35 of which have

162   E-boxes in their regulatory regions, were also decreased in myc^{P0} mutant ovaries,

163   suggesting that secondary transcriptional controls might also be involved in Myc's

164   regulation on mitochondrial biogenesis.

165

166   **IIS regulates Myc post-transcriptionally through Sgg and Thor**

167   Having identified Myc as the master regulator of ETC biogenies and mtDNA

168   replication in the ovary, we sought to explore how the spatial-temporal pattern of Myc

169   protein was established. Myc can be regulated either transcriptionally or post-

170   transcriptionally by a variety of upstream signals (Gallant, 2013). We first examined *myc*

171   transcription by visualizing its promoter activity using a *myc-LacZ* transgene (Neto-Silva

172   et al., 2010). In contrast to Myc protein, which was markedly up-regulated at region 2B,

173   *myc* transcript appeared to be uniform in the germarium (Fig 2B), suggesting that post-

174   transcriptional regulations are responsible for the spatial pattern of Myc protein.

175   IIS/TORC1 signaling is known to regulate both translation and protein stability

176   (Garofalo, 2002; Maurer et al., 2014; Pan et al., 2004), and multiple genes in the

177   IIS/TORC1 signaling emerged from the initial RNAi screen. Consistently, ETC activity

178   and mtDNA replication was severely impaired in ovaries of *chico* mutant flies (Fig 3A-

179   3C), which obtained by combing two *chico* mutant alleles, *chico^1* (loss of function) and

180   *chico^{KG}* (hypomorphic) (Bohni et al., 1999; Song et al., 2010). These data support a

181   critical role of IIS in ETC biogenesis and mtDNA replication. Intriguingly, the activity of

182   IIS, revealed by staining for phosphorylated AKT (p-AKT) (Parker and Struhl, 2015),

183   was also increased in the germarium region 2B and maintained until mid-stage egg

184   chambers (Fig 3D and S3A), a pattern similar to that of Myc protein. In contrast, total

185   AKT staining was uniform in the germarium (Fig 3D). These observations suggest that

186   Myc may be regulated by IIS. Indeed, Myc protein was strongly reduced in *chico$^{1/KG}$*

187   mutant ovaries (Fig 3E and 3F). In *chico* RNAi ovaries, Myc protein was also diminished

188   in germ cells, while the expression of *myc-LacZ* was not affected (Fig 4B and S4A).

189   Importantly, over-expressing Myc in the *chico* RNAi background largely restored ETC

190   biogenesis in the ovary (Fig 4D). Altogether, these results suggest that up-regulation of

191   IIS in late germarium stimulates ETC biogenesis and mtDNA replication through post-

192   transcriptional control of Myc level.

193   Next, we explored how IIS regulates Myc. IIS either promotes protein translation

194   by repressing 4E-BP/Thor, or stabilizes its targets by antagonizing GSK3/Sgg

195   dependent protein degradation (Fig 4A) (Garofalo, 2002; Maurer et al., 2014; Pan et al.,

196   2004). Knocking down of *sgg* in a *chico* RNAi background restored Myc protein level

197   and ETC activity, while *thor* RNAi only partially rescued both (Fig 4B-4D). Intriguingly,

198   *sgg* RNAi not only elevated Myc protein level in region 2B and thereafter, but also

199   strongly induced Myc in earlier stages where Myc protein is not normally present (Fig

200   4E and 4F). Next, we examined the pattern of GSK3 and GSK3 activity in the

201   germarium. GSK3 activity is suppressed by IIS through AKT phosphorylation on GSK3

202   Ser9. GSK3 protein visualized by both antibody staining and an endogenous expressed

203   Sgg-GFP was ubiquitous throughout oogenesis (Fig 4G and S4F). However,

204   phosphorylated GSK3, the inactive form of GSK3, became evident in region 2B

205   germarium and later stages egg chambers, the same pattern as p-AKT, Myc, and ETC

206   biogenesis (Fig 1B, 3F, 4G, and S4C). Taken together, these data suggest that Sgg is

207   the main regulator of Myc and acts downstream of IIS.

208

InR expression is boosted at region 2B germarium

210   So far, our data has established Myc as the link between IIS, a major pathway
211 regulating cell proliferation and growth, and mitochondrial biogenesis in ovaries. The IIS
212 regulates germ cells growth and proliferation in response to insulin-like peptides (dilps)
213 produced by neuroendocrine cells (LaFever and Drummond-Barbosa, 2005). *Drosophila*
214 has an open circulatory system. In a given tissue, all cells are exposed to a similar level
215 of dilps circulating in the hemolymph. However, instead of being uniform in the
216 germarium, the activity of IIS, indicated by both p-AKT and inhibitory phosphorylated
217 Sgg staining (Fig 3D and 4G), demonstrated a distinct spatial-temporal pattern similar to
218 that of Myc, ETC expression and mtDNA replication. Therefore, some IIS components
219 downstream of dilps are likely differentially expressed in germarium.

220   To test this idea, we generated an InR-EGFP reporter line by inserting an EGFP
221 at the C-terminus of the *InR* genomic locus. Using this line and other reporter lines
222 (Nagarkar-Jaiswal et al., 2015; Orme et al., 2006; Sarov et al., 2016), we examined the
223 expression patterns of InR and other components of IIS signaling upstream of AKT. InR-
224 EGFP was upregulated in region 2B (Fig 4H), while all other components in the IIS
225 signaling examined were ubiquitously expressed in the germarium (Fig S5A).
226 Additionally, *InR* mRNA, visualized by FISH, demonstrated the same pattern as that of
227 InR-EGFP (Fig 4H), suggesting that up-regulation of *InR* transcription enhances IIS to
228 boost mitochondrial biogenesis.

229

Both JNK pathway and Myc promote IIS activity via *InR* transcription

231   We next asked how *InR* transcription was elevated at region 2B germarium. The
232 JNK pathway, which transcriptionally controls various cellular processes (Weston and
233 Davis, 2007), had emerged from the initial RNAi screen. Consistent with the RNAi
234 screen, homozygous *bsk^1* clones showed impaired mtDNA replication, compared to
235 *bsk^1/+* heterozygous germ cells (Fig 5A and 5B). Interestingly, JNK signaling activity,
236 visualized by a *puc-LacZ* reporter (Martin-Blanco et al., 1998), was sharply up-regulated
237 in late germarium stages, but deceased and eventually disappeared in growing egg
238 chambers (Fig 5C and S5B). The partial overlap between the spatial patterns of IIS and

239 JNK activation, and the phenotypic resemblance between IIS and JNK mutations on
240 ETC activities and mtDNA replication, suggest a potential link between these two
241 pathways. Indeed, IIS activity, Myc protein, and *InR* mRNA were all markedly reduced in
242 ovaries expressing dsRNA against either *bsk* or *jra*, fly homolog of JNK or Jun,
243 respectively (Fig 5D-5I and S5C-S5E). In *bsk* RNAi or *jra* RNAi background, over-
244 expression of *InR* restored Myc level and over-expression of either *InR* or *Myc* rescues
245 ETC activity (Fig 5H and 5I). In contrast, enhancing JNK signaling by *puc* RNAi failed to
246 rescue defective ETC activity in a *chico* RNAi background (Fig 5I). Together, these
247 observations suggest that JNK promotes ETC biogenesis in late germarium stages
248 thorough boosting IIS.

249   IIS was elevated in region 2B and remained active until stage-10 egg chambers,
250 the same period during which ETC biogenesis and mtDNA replication are active.
251 However, JNK is only transiently activated at region 2B. Therefore, additional
252 regulations must be involved to maintain IIS activity after JNK activity subsides. Our
253 RNAseq results showed that *InR* mRNA was down-regulated in the myc^{P0} ovary
254 compared with controls (Table S2), suggesting that Myc might activate *InR* transcription.
255 Indeed, both *InR* mRNA level measured by FISH and IIS activity indicated by p-AKT
256 were reduced in myc^{P0} mutant or *chico* RNAi ovaries (Fig 6A-6D, S6A, and S6B).
257 Significantly, over-expression of *myc* using *bam*-Gal4 in region 2A ectopically induced
258 *InR* transcription and IIS activity (Fig 6A-6D, S6A, and S6B), suggesting that Myc can
259 indeed enhance IIS by boosting *InR* expression. Together, our results highlight an IIS-
260 Myc positive feedback loop that promotes ETC biogenesis and mtDNA replication in the
261 ovary.

262

263 **The JNK-IIS-Myc relay is essential for female fertility and mtDNA selective**
264 **inheritance**

265   So far we have established that the JNK-IIS-Myc relay is critical for ETC activity,
266 mtDNA expression, replication, and inheritance in the ovary. Next, we explored its
267 physiological impact on reproduction. While both *chico* mutant females and those with
268 germline clones of bsk^{1} produced similar amount of eggs as control, they failed to

269 generate adequate amount of mtDNA to deposit in eggs (Fig 7A). Thus, their eggs had

270 significantly reduced mtDNA level and hatching rates (Fig 7B).

271 During oogenesis, the wild-type mitochondrial genomes enriched in healthy

272 mitochondria out-compete lethally mutated mtDNA afflicting defective mitochondria (Hill

273 et al., 2014). Thus, we asked whether abolishing IIS and JNK signaling would impair

274 mtDNA selective inheritance in heteroplasmic females harboring both wt and a

275 temperature-sensitive lethal mutation, *mt:Col^{T300I}* (Hill et al., 2014). Consistent with

276 previous studies, eggs contain ~20% less *mt:Col^{T300I}* mtDNA on average than their

277 mothers at a restrictive temperature (Fig 7C). However, down-regulation of either IIS or

278 JNK signaling abolished the counter-selection of *mt:Col^{T300I}* genome (Fig 7C). Together,

279 these results stress that although JNK is transiently activated in the late germarium, it

280 triggers a developmental signaling relay that has profound impacts on mitochondrial

281 inheritance through activation of ETC biogenesis and mtDNA replication.

282

DISCUSSION

283

284 mtDNA replication in the *Drosophila* ovary relies on active respiration (Hill et al.,

285 2014), suggesting that ETC activity might be subject to the same spatial-temporal

286 regulation as mtDNA replication. In this study, we address this question and further

287 elucidate the underlying developmental regulations of ETC activity and mtDNA

288 biogenesis in ovary. We reveal that ETC complexes, exemplified by COX/SDH are

289 inactive in the GSCs and dividing cysts from germarium region 1 to 2A, but sharply

290 activated in region 2B, and remain active until stage 10 follicles, in which a metabolic

291 reprograming takes place (Sieber et al., 2016). This spatial pattern mirrors that of

292 mtDNA replication in the *Drosophila* ovary, further substantiating an essential role of

293 mitochondrial respiration in mtDNA inheritance, both quantitively and qualitatively. We

294 also demonstrate that the ETC activation is accompanied with an upregulation of the

295 expression of ETC genes on both nuclear and mitochondrial genomes. Interestingly,

296 MDI that drives the local translation of nuclear encoded mitochondrial proteins on the

297 mitochondrial outer membrane and TFAM that governs mtDNA replication and

298 transcription (Falkenberg et al., 2007; Zhang et al., 2016), exhibit the same

299 developmental pattern as mitochondrial respiration in the germarium. Collectively, these

300 proteins would boost the biogenesis of ETC in region 2B germarium and growing egg

301 chambers. In an ovariole, different stages of developing germ cells reside in the same

302 microenvironment and experience same oxygen tension. Thus, the mitochondrial

303 respiratory activity is likely to be determined by the abundance of ETC, which is

304 controlled by transcriptional activation.

305 To understand how ETC biogenesis is regulated, we conducted a candidate

306 RNAi screening for genes that are required for boosting COX/SDH activities in ovary.

307 Myc emerged as one of the strongest hits, and a hypermorphic allele of myc^{P0} largely

308 abolished ETC activities and mtDNA replication in the germarium. Moreover, the spatial

309 pattern of Myc protein mirrors mtDNA replication and ETC activity, further supporting its

310 essential role in transcriptional activation of ETC biogenesis. RNA sequencing data

311 demonstrate that Myc broadly stimulates the gene expression in the *Drosophila* ovary,

312 including many nuclear encoded ETC genes and factors required for mtDNA replication

313 and expression. Our results are consistent with studies on mammal cultured cells

314 showing that Myc can stimulate mitochondrial genes expression and enhance

315 mitochondrial respiration (Li et al., 2005; Stine et al., 2015). Myc overexpression in

316 different cell types or different conditions, sometimes give rise to different transcriptional

317 output (de la Cova et al., 2014). These observations underscore that Myc family

318 proteins often associate with other cofactors and exert a broad and complex

319 transcriptional activation or repression in a cell/tissue specific manner (Cowling and

320 Cole, 2006; Hann, 2014). We also found that 130 transcription regulators, including *Srl*

321 (fly homolog of human PGC-1) and CG32343 (fly homolog of GABPB2), were affected

322 in the *myc^{P0}* ovary. PGC-1 proteins belong to an evolutionarily conserved family that

323 integrates mitochondrial biogenesis and energy metabolism with a variety of cellular

324 processes (Lin et al., 2005). In *Drosophila*, *Srl* regulates the expression of a subset of

325 nuclear encoded mitochondrial genes (Tiefenbock et al., 2010). Mammalian GABPB2 is

326 a regulatory subunit of the Nuclear Respiratory Factor 2 complex that regulates the

327 expression of a small set of nuclear encoded mitochondrial proteins (Kelly and

328 Scarpulla, 2004). Therefore, additional tiers of transcriptional regulations downstream of

329 Myc are likely involved to boost ETC biogenesis.

330   While *myc* transcription is uniform in the germarium, Myc protein is elevated at

331 region 2B and remained at high level until the stage 10 egg chamber, highlighting that

332 Myc protein level is mainly regulated *via* post transcriptional mechanisms,. IIS and JNK

333 also emerged from our candidate screening, and both were further confirmed to be

334 required for triggering ETC biogenesis and mtDNA replication. We found that IIS

335 activity, marked by both p-AKT and p-GSK3 staining, displayed a similar pattern to that

336 of Myc. Additionally, elevated IIS activity was required to establish a high level of Myc

337 and to activate ETC in late germarium stage. Our result is line with a previous study

338 showing that decreased IIS activity relieves the inhibition on GSK3, which leads to

339 mitochondrial quiescence at later stages of oogenesis (Sieber et al., 2016). Importantly,

340 our work uncovers Myc as the downstream effector of IIS on the regulation of

341 respiration and mtDNA biogenesis in the ovary.

342   We noticed that *InR* transcription was down-regulated in the *myc* mutant ovary,

343 suggesting a positive feedback regulation between IIS and Myc. This regulatory loop

344 maintains high levels of both Myc protein and IIS in the mid-stage follicles, where

345   prodigious mitochondrial biogenesis and massive cell growth take place. However, it

346   does not explain how this loop is activated in the first place at the late germarium

347   stages. We found that JNK was transiently activated in germ cells at the germarium 2B,

348   but decreased in budding egg chambers and sharply diminished thereafter. High level

349   and sustained JNK activity often leads to apoptosis. However, cell death is rarely

350   observed in germaria of flies cultured under the normal condition. Thus, temporal JNK

351   activation at late germarium must be associated with other cellular processes. We

352   reveal that transiently-elevated JNK activity is sufficient to increase *InR* mRNA level,

353   which in-turn boosts IIS and stabilizes Myc protein. Currently, the potential link between

354   JNK and IIS is well-understood. The metastatic *Drosophila* epithelium cells require JNK

355   to up-regulate *InR* expression through wingless signaling to promote cell survival and

356   proliferation (Hirabayashi et al., 2013). However, no genes in wingless signaling

357   emerged from our RNAi screening in germ cells. Molecular mechanisms that links JNK

358   activation to *InR* expression in ovary remains to be explored.

359   JNK-dependent transcriptional program can be activated by various cellular

360   stresses and cell-cell signaling (Rios-Barrera and Riesgo-Escovar, 2013). In region 2B

361   germarium, the follicle cells extend and migrate laterally across the germarium to wrap

362   around the 16-cells cyst (Nystul and Spradling, 2007). Thus, follicle cells may active

363   JNK in germ cells through paracrine signals, such as TNF-α. Alternatively, the process

364   of follicle cells enveloping and compressing the 16-cell cyst may generate mechanical

365   stresses that subsequently activates JNK. Regardless, our work uncovers a novel

366   function of JNK in energy metabolism and mitochondrial biogenesis besides its well

367   established roles in controlling cell apoptosis, growth, and proliferation.

368   Studies in a variety of animal models have showed that reproductive aging of

369   females is tightly associated with decreased IIS (Templeman and Murphy, 2018).

370   Interestingly, oocytes of aged females often have higher incidence of mtDNA lesions

371   and lower mtDNA copy number (Chan et al., 2005). Thus, our findings on

372   developmental control of mitochondrial biogenesis and mtDNA replication via IIS may

373   be a conserved mechanism in metazoans. Our studies could be a molecular framework

374   to further understand the control of mitochondrial biogenesis and mtDNA inheritance in

375   animals.

376

STAR☐METHODS

Detailed methods are provided in the online version of this paper and include the following:

- **KEY RESOURCES TABLE**
- **CONTACT FOR REAGENT AND RESOURCE SHARING**
- **EXPERIMENTAL MODEL AND SUBJECT DETAILS**
- **METHODS DETAILS**
- **QUANTIFICATION AND STATISTICAL ANALYSIS**
- **DATA AVAILABILITY**

SUPPLEMENTAL INFORMATION

Supplemental Information includes seven figures and three tables.

ACKNOWLEDGEMENTS

AUTHOR CONTRIBUTIONS

Z-H.W. and H.X. conceived the project and design the experiments. Z-H.W. and Y.L. performed the experiments. Z-H.W., V.C., M.P. and H. X. analyzed data. Z-H.W. and H.X. wrote the paper.

DECLARATION OF INTERESTS

The authors declare no competing interests.

REFERENCE

Basson, M.A. (2012). Signaling in cell differentiation and morphogenesis. Cold Spring Harb Perspect Biol *4*.

Bohni, R., Riesgo-Escovar, J., Oldham, S., Brogiolo, W., Stocker, H., Andruss, B.F., Beckingham, K., and Hafen, E. (1999). Autonomous control of cell and organ size by CHICO, a Drosophila homolog of vertebrate IRS1-4. Cell *97*, 865-875.

Chan, C.C., Liu, V.W., Lau, E.Y., Yeung, W.S., Ng, E.H., and Ho, P.C. (2005). Mitochondrial DNA content and 4977 bp deletion in unfertilized oocytes. Mol Hum Reprod *11*, 843-846.

Claveria, C., and Torres, M. (2016). Cell Competition: Mechanisms and Physiological Roles. Annu Rev Cell Dev Biol *32*, 411-439.

Cowling, V.H., and Cole, M.D. (2006). Mechanism of transcriptional activation by the Myc oncoproteins. Semin Cancer Biol *16*, 242-252.

de la Cova, C., Senoo-Matsuda, N., Ziosi, M., Wu, D.C., Bellosta, P., Quinzii, C.M., and Johnston, L.A. (2014). Supercompetitor status of Drosophila Myc cells requires p53 as a fitness sensor to reprogram metabolism and promote viability. Cell Metab *19*, 470-483.

Desvergne, B., Michalik, L., and Wahli, W. (2006). Transcriptional regulation of metabolism. Physiol Rev *86*, 465-514.

Falkenberg, M., Larsson, N.G., and Gustafsson, C.M. (2007). DNA replication and transcription in mammalian mitochondria. Annu Rev Biochem *76*, 679-699.

Gallant, P. (2013). Myc function in Drosophila. Cold Spring Harb Perspect Med *3*, a014324.

Garofalo, R.S. (2002). Genetic analysis of insulin signaling in Drosophila. Trends Endocrinol Metab *13*, 156-162.

Greer, C., Lee, M., Westerhof, M., Milholland, B., Spokony, R., Vijg, J., and Secombe, J. (2013). Myc-dependent genome instability and lifespan in Drosophila. PLoS One *8*, e74641.

Hann, S.R. (2014). MYC cofactors: molecular switches controlling diverse biological outcomes. Cold Spring Harb Perspect Med *4*, a014399.

435   Hill, J.H., Chen, Z., and Xu, H. (2014). Selective propagation of functional mitochondrial
436   DNA during oogenesis restricts the transmission of a deleterious mitochondrial variant.
437   Nat Genet *46*, 389-392.

438   Hirabayashi, S., Baranski, T.J., and Cagan, R.L. (2013). Transformed Drosophila cells
439   evade diet-mediated insulin resistance through wingless signaling. Cell *154*, 664-675.

440   Johnston, L.A., Prober, D.A., Edgar, B.A., Eisenman, R.N., and Gallant, P. (1999).
441   Drosophila myc regulates cellular growth during development. Cell *98*, 779-790.

442   Kelly, D.P., and Scarpulla, R.C. (2004). Transcriptional regulatory circuits controlling
443   mitochondrial biogenesis and function. Genes Dev *18*, 357-368.

444   LaFever, L., and Drummond-Barbosa, D. (2005). Direct control of germline stem cell
445   division and cyst growth by neural insulin in Drosophila. Science *309*, 1071-1073.

446   Li, F., Wang, Y., Zeller, K.I., Potter, J.J., Wonsey, D.R., O'Donnell, K.A., Kim, J.W.,
447   Yustein, J.T., Lee, L.A., and Dang, C.V. (2005). Myc stimulates nuclearly encoded
448   mitochondrial genes and mitochondrial biogenesis. Mol Cell Biol *25*, 6225-6234.

449   Lin, J., Handschin, C., and Spiegelman, B.M. (2005). Metabolic control through the
450   PGC-1 family of transcription coactivators. Cell Metab *1*, 361-370.

451   Martin-Blanco, E., Gampel, A., Ring, J., Virdee, K., Kirov, N., Tolkovsky, A.M., and
452   Martinez-Arias, A. (1998). puckered encodes a phosphatase that mediates a feedback
453   loop regulating JNK activity during dorsal closure in Drosophila. Genes Dev *12*, 557-
454   570.

455   Maurer, U., Preiss, F., Brauns-Schubert, P., Schlicher, L., and Charvet, C. (2014). GSK-
456   3 - at the crossroads of cell death and survival. J Cell Sci *127*, 1369-1378.

457   May-Panloup, P., Chretien, M.F., Malthiery, Y., and Reynier, P. (2007). Mitochondrial
458   DNA in the oocyte and the developing embryo. Curr Top Dev Biol *77*, 51-83.

459   Nagarkar-Jaiswal, S., Lee, P.T., Campbell, M.E., Chen, K., Anguiano-Zarate, S.,
460   Gutierrez, M.C., Busby, T., Lin, W.W., He, Y., Schulze, K.L., et al. (2015). A library of
461   MiMICs allows tagging of genes and reversible, spatial and temporal knockdown of
462   proteins in Drosophila. Elife *4*.

463   Neto-Silva, R.M., de Beco, S., and Johnston, L.A. (2010). Evidence for a Growth-
464   Stabilizing Regulatory Feedback Mechanism between Myc and Yorkie, the Drosophila
465   Homolog of Yap. Dev Cell *19*, 507-520.

466 Nystul, T., and Spradling, A. (2007). An epithelial niche in the Drosophila ovary
467 undergoes long-range stem cell replacement. Cell Stem Cell *1*, 277-285.

468 Oldham, S., and Hafen, E. (2003). Insulin/IGF and target of rapamycin signaling: a TOR
469 de force in growth control. Trends Cell Biol *13*, 79-85.

470 Orian, A., van Steensel, B., Delrow, J., Bussemaker, H.J., Li, L., Sawado, T., Williams,
471 E., Loo, L.W., Cowley, S.M., Yost, C., et al. (2003). Genomic binding by the Drosophila
472 Myc, Max, Mad/Mnt transcription factor network. Genes Dev *17*, 1101-1114.

473 Orme, M.H., Alrubaie, S., Bradley, G.L., Walker, C.D., and Leevers, S.J. (2006). Input
474 from Ras is required for maximal PI(3)K signalling in Drosophila. Nat Cell Biol *8*, 1298-
475 1302.

476 Pan, D., Dong, J., Zhang, Y., and Gao, X. (2004). Tuberous sclerosis complex: from
477 Drosophila to human disease. Trends Cell Biol *14*, 78-85.

478 Parker, J., and Struhl, G. (2015). Scaling the Drosophila Wing: TOR-Dependent Target
479 Gene Access by the Hippo Pathway Transducer Yorkie. PLoS Biol *13*, e1002274.

480 Perrimon, N., Pitsouli, C., and Shilo, B.Z. (2012). Signaling mechanisms controlling cell
481 fate and embryonic patterning. Cold Spring Harb Perspect Biol *4*, a005975.

482 Pesole, G., Gissi, C., De Chirico, A., and Saccone, C. (1999). Nucleotide substitution
483 rate of mammalian mitochondrial genomes. J Mol Evol *48*, 427-434.

484 Picton, H., Briggs, D., and Gosden, R. (1998). The molecular basis of oocyte growth
485 and development. Mol Cell Endocrinol *145*, 27-37.

486 Quinn, L.M., Dickins, R.A., Coombe, M., Hime, G.R., Bowtell, D.D., and Richardson, H.
487 (2004). Drosophila Hfp negatively regulates dmyc and stg to inhibit cell proliferation.
488 Development *131*, 1411-1423.

489 Ren, Q., Zhang, F., and Xu, H. (2017). Proliferation Cycle Causes Age Dependent
490 Mitochondrial Deficiencies and Contributes to the Aging of Stem Cells. Genes (Basel) *8*.

491 Rios-Barrera, L.D., and Riesgo-Escovar, J.R. (2013). Regulating cell morphogenesis:
492 the Drosophila Jun N-terminal kinase pathway. Genesis *51*, 147-162.

493 Sarov, M., Barz, C., Jambor, H., Hein, M.Y., Schmied, C., Suchold, D., Stender, B.,
494 Janosch, S., K, J.V., Krishnan, R.T., et al. (2016). A genome-wide resource for the
495 analysis of protein localisation in Drosophila. Elife *5*, e12068.

496   Sieber, M.H., Thomsen, M.B., and Spradling, A.C. (2016). Electron Transport Chain
497   Remodeling by GSK3 during Oogenesis Connects Nutrient State to Reproduction. Cell
498   *164*, 420-432.

499   Song, W., Ren, D., Li, W., Jiang, L., Cho, K.W., Huang, P., Fan, C., Song, Y., Liu, Y.,
500   and Rui, L. (2010). SH2B regulation of growth, metabolism, and longevity in both
501   insects and mammals. Cell Metab *11*, 427-437.

502   Stewart, J.B., Freyer, C., Elson, J.L., and Larsson, N.G. (2008). Purifying selection of
503   mtDNA and its implications for understanding evolution and mitochondrial disease. Nat
504   Rev Genet *9*, 657-662.

505   Stewart, J.B., and Larsson, N.G. (2014). Keeping mtDNA in shape between
506   generations. PLoS Genet *10*, e1004670.

507   Stine, Z.E., Walton, Z.E., Altman, B.J., Hsieh, A.L., and Dang, C.V. (2015). MYC,
508   Metabolism, and Cancer. Cancer Discov *5*, 1024-1039.

509   Stump, C.S., Short, K.R., Bigelow, M.L., Schimke, J.M., and Nair, K.S. (2003). Effect of
510   insulin on human skeletal muscle mitochondrial ATP production, protein synthesis, and
511   mRNA transcripts. Proc Natl Acad Sci U S A *100*, 7996-8001.

512   Templeman, N.M., and Murphy, C.T. (2018). Regulation of reproduction and longevity
513   by nutrient-sensing pathways. J Cell Biol *217*, 93-106.

514   Tiefenbock, S.K., Baltzer, C., Egli, N.A., and Frei, C. (2010). The Drosophila PGC-1
515   homologue Spargel coordinates mitochondrial activity to insulin signalling. EMBO J *29*,
516   171-183.

517   Wallace, D.C. (2008). Mitochondria as chi. Genetics *179*, 727-735.

518   Weston, C.R., and Davis, R.J. (2007). The JNK signal transduction pathway. Curr Opin
519   Cell Biol *19*, 142-149.

520   Zhang, Y., Chen, Y., Gucek, M., and Xu, H. (2016). The mitochondrial outer membrane
521   protein MDI promotes local protein synthesis and mtDNA replication. EMBO J *35*, 1045-
522   1057.

523   Zhang, Y., Wang, Z.H., Liu, Y., Chen, Y., Sun, N., Gucek, M., Zhang, F., and Xu, H.
524   (2019). PINK1 Inhibits Local Protein Synthesis to Limit Transmission of Deleterious
525   Mitochondrial DNA Mutations. Mol Cell *73*, 1127-1137 e1125.

526

527   **Figures and Figure Legends**

528   **Figure 1**
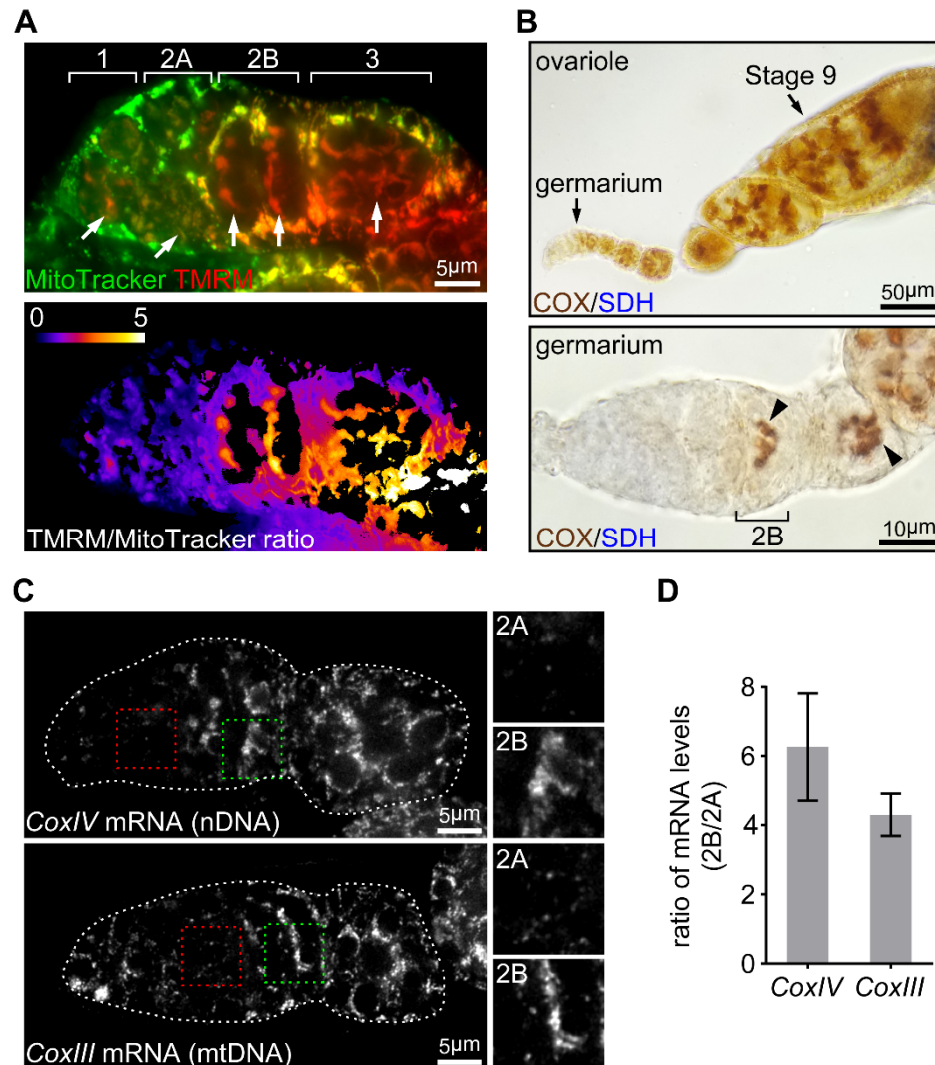

529

530   **Figure 1. ETC activity and gene expression sharply increase at germarium stage**

531   **2B.**

532   (A) Upper panel: a representative image of a germarium stained with TMRM (a

533   membrane potential marker) and MitoTracker Green (a mitochondrial mass marker).

534   Germarium regions are indicated. Arrows indicate mitochondria in germ cells (GCs).

535   Lower panel: TMRM/MitoTracker Green ratiometric image, indicating that mitochondria

536   membrane in in stem cells and dividing cysts is low, but markedly increased in 16 cell

537   cysts and budding egg chambers.

538 (B) Upper panel: a representative image of a wt ovariole (from germarium to stage 9

539 egg chamber) stained for the COX/SDH dual activities. Lower panel: a representative

540 high-magnification image of a germarium stained for COX/SDH. Note the onset of

541 COX/SDH activity in region 2B of the germarium (arrowhead).

542 (C) Visualization of the *CoxIV* and *CoxIII* mRNA in germaria from wt flies with

543 fluorescently labelled DNA probes by FISH. Germaria are outlined with dotted lines.

544 Right panels illustrate the enlarged areas of germarium region 2A (red dotted line) and

545 2B (green dotted line), respectively, shown in left panels.

546 (D) Quantification for the relative expression level of *CoxIV* or *CoxIII* mRNA in different

547 regions of germarium. Note that both transcripts are markedly induced in region 2B

548 germarium.

549

Wang et al., 2019

Figure 2

G Catagory of decreased mRNAs in myc^{P0} ovaries

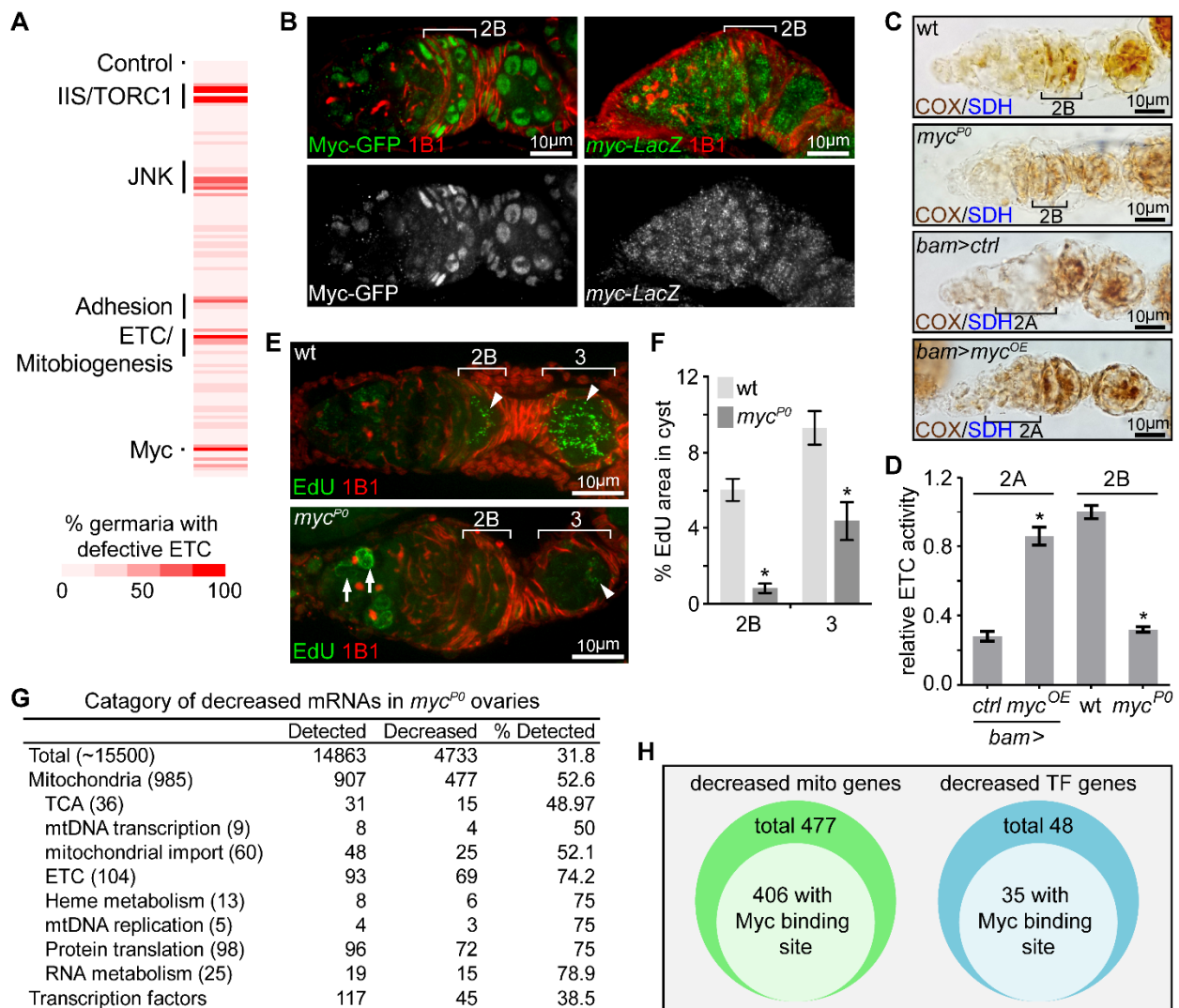|	Detected	Decreased	% Detected
Total (~15500)	14863	4733	31.8
Mitochondria (985)	907	477	52.6
TCA (36)	31	15	48.97
mtDNA transcription (9)	8	4	50
mitochondrial import (60)	48	25	52.1
ETC (104)	93	69	74.2
Heme metabolism (13)	8	6	75
mtDNA replication (5)	4	3	75
Protein translation (98)	96	72	75
RNA metabolism (25)	19	15	78.9
Transcription factors	117	45	38.5

Figure 2. A candidate RNAi screen reveals Myc as an essential regulator for mitochondrial biogenesis.

(A) RNAi screening for genes that are required for inducing ETC activity in germaria. For each line, the impact on ETC activity is scored as the percentage of germaria with reduced COX/SDH staining.

(B) Left panel: a germarium from flies endogenously expressing Myc-GFP stained with anti-GFP (Green) and anti-1B1 (Red). Right panel: a germarium flies expressing LacZ driven by *myc* endogenous promoter stained with anti-β-galactosidase (Green) and anti-1B1 (Red). Myc protein is expressed in low level in GSCs and dividing cysts, but

22

561 markedly induced from region 2B germ cells. In contrast, Myc promoter activity is
562 uniform in the germarium.

563 (C) ETC activity in germaria from wt, *myc^{P0}*, *bam>ctrl*, and *bam>myc^{OE}* ovaries
564 visualized by COX/SDH staining. ETC activity is significantly reduced in the *myc^{P0}*
565 mutant, but is ectopically induced when Myc is over-expressed in region 2A by *bam-*
566 Gal4.

567 (D) Quantification of relative ETC activity in germarium regions from ovaries with
568 indicated genotypes. ETC activity is normalized to that in the wt 2B cysts.

569 (E) Visualization of mtDNA replication in germaria from wt and *myc^{P0}* ovaries with EdU
570 incorporation (Green) and co-stained with anti-1B1 (Red). Arrows indicate mtDNA
571 replication, while arrowheads point out EdU incorporation into the nuclear genome.

572 (F) Area of EdU puncta (pixels) is normalized to total pixels germline cysts at indicated
573 germarium stages from wt and *myc^{P0}* ovaries.

574 (G) Table of genes functioning in mitochondrial processes with at least 3-fold decreased
575 expression in *myc^{P0}* ovaries compared with wt ovaries.

576 (H) Diagrams of decreased genes encoding mitochondrial processes and TFs in the
577 *myc^{P0}* ovaries. A number of genes in either category has Myc binding site in their
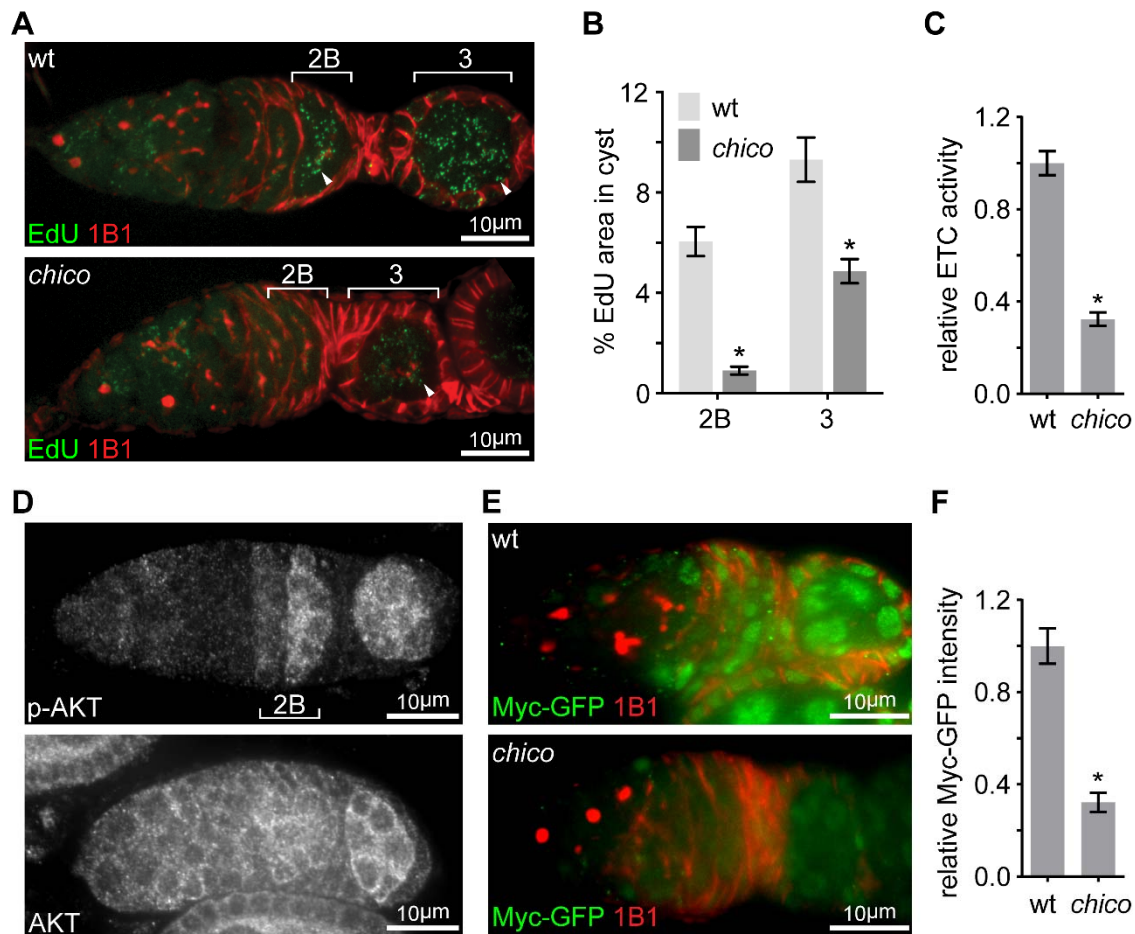578 regulatory region.

579 Error bars represent SEM. *$p < 0.005$.

580

Wang et al., 2019

581   **Figure 3**

582

583   **Figure 3. Elevated IIS in late germarium induces Myc protein to prime mtDNA**
584   **replication and mitochondrial respiration.**

585   (A) Representative germaria from wt or *chico*[1/KG] mutant flies incorporating EdU stained
586   with anti-1B1. Arrowheads indicate EdU incorporation into mtDNA of germ cells.

587   (B) Quantification of the percentage of EdU area in germline cysts from wt or *chico*[1/KG]
588   mutant flies.

589   (C) Quantification of relative ETC activity in region 2B cysts from wt or *chico*[1/KG] mutant
590   flies.

591   (D) Germaria from wt ovaries stained with anti-AKT and anti-p-AKT, respectively. p-AKT
592   staining is low in both GSCs and dividing cysts, but increased from region 2B germ
593   cells. In contrast, AKT staining is uniform in the germarium.

24

594   (E) Germaria from wt or *chico^{1/KG}* mutant ovaries endogenously expressing Myc-GFP

595   stained with anti-GFP, anti-1B1, and DAPI. Germarium region 2B is underlined with

596   dotted lines.

597   (F) Quantification of relative Myc-GFP intensity in germarium region 2B from wt or

598   *chico^{1/KG}* mutant ovaries.

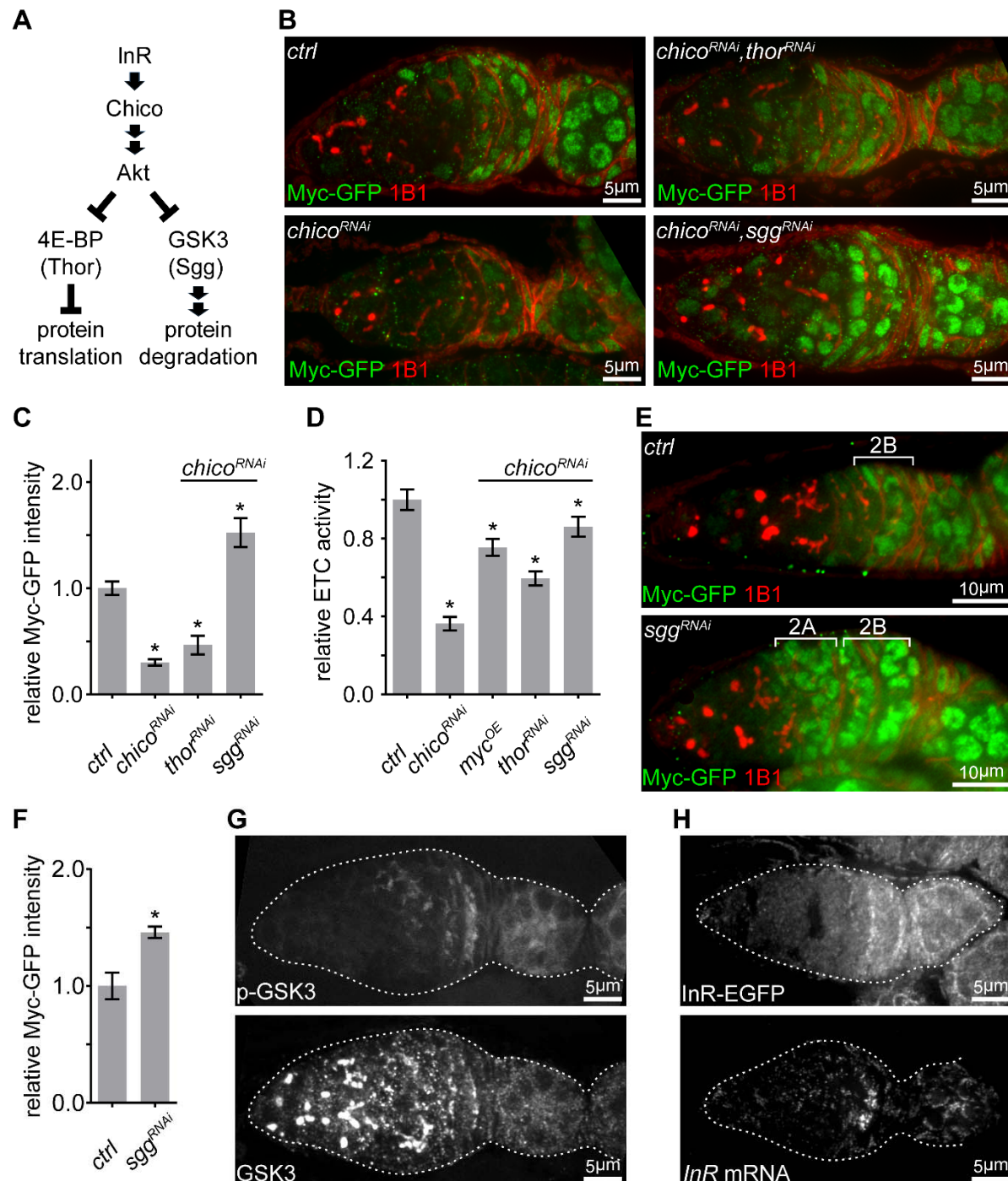599   Error bars represent SEM. *p < 0.005.

Figure 4

Figure 4. IIS promotes ETC activity via inhibition of GSK3 to stabilize Myc.

(A) Schematic of the conserved IIS that inhibits 4E-BP/Thor and GSK3/Sgg to promote

protein translation and suppress protein degradation, respectively.

26

605 (B) Germaria from *nos>ctrl*; *nos>chico^{RNAi}*; *nos>chico^{RNAi}*, *thor^{RNAi}*; and *nos>chico^{RNAi}*,

606 *sgg^{RNAi}* ovaries endogenously expressing Myc-GFP stained with anti-GFP (green) and

607 anti-1B1 (red). Germ cells from region 2B are outlined with dotted lines.

608 (C, D) Quantification of Myc-GFP intensity (C) and ETC activity (D) in germarium region

609 2B from ovaries with indicated genotypes, normalized to the intensity or activity values

610 in germaria with *ctrl* over-expression.

611 (E) Germaria from *nos>ctrl* and *nos>sgg^{RNAi}* ovaries endogenously expressing Myc-

612 GFP stained with anti-GFP and anti-1B1. Myc protein is up-regulated in both region 2A

613 and region 2B germ cells in the *sgg* RNAi ovary.

614 (F) Quantification of relative Myc-GFP intensity in germarium region 2B from *nos>ctrl*

615 and *nos>sgg^{RNAi}* ovaries. Myc-GFP intensity is normalized to that of region 2B cysts

616 with *ctrl* over-expression.

617 (G) A germarium from wt flies stained with anti-GSK3 and anti-p-GSK3. Germaria are

618 outlined with dotted lines.

619 (H) Upper panel: a representative image of a germarium from ovaries expressing

620 endogenous InR-EGFP. Lower panel: visualization of the *InR* mRNA in germarium with

621 fluorescently labelled DNA probes by FISH. Germaria are outlined with dotted lines.

622 Error bars represent SEM. *$p < 0.005$.

Figure 5

Figure 5. Transient JNK activation in the germarium boosts the IIS-Myc signaling.

(A) Representative germaria with *bsk[1]* FRT clones with EdU incorporation (green) to visualize mtDNA replication. *bsk[1]/+* cells are positive for mRFP (red), while *bsk[1]* mutant cells are negative for mRFP. Arrows indicate EdU incorporated into mtDNA, while arrowheads point out EdU incorporated into the nuclear genome.

(B) The percentage area of EdU incorporated into mtDNA in germline cysts at indicated germarium stages from *bsk[1]/+* and *bsk[1]* clones.

632   (C) Germarium from ovaries expressing LacZ driven by the *puc* promoter stained with

633   anti-β-galactosidase (green) and anti-Vasa (red). Germarium is outlined with dotted

634   lines.

635   (D) Germaria from *nos>ctrl* and *nos>bsk^{RNAi}* flies stained with anti-p-AKT (green) and

636   anti-1B1 (red). Note that IIS activity is markedly reduced when JNK signaling is

637   decreased by *bsk* RNAi.

638   (E) Quantification of p-AKT intensity from cysts in germarium region 2A and 2B of

639   ovaries with indicated genotypes. p-AKT intensity is normalized to that of region 2B

640   cysts from the *ctrl* line.

641   (F) Visualization of the *InR* mRNA by FISH in germaria from *nos>ctrl* and *nos>bsk^{RNAi}*

642   ovaries co-stained with DAPI. Note that *InR* mRNA level is decreased by *bsk* RNAi.

643   Germaria are outlined with dotted lines.

644   (G) Quantification of *InR* mRNA density in region 2B germ cells from ovaries with

645   indicated genotypes.

646   (H) Germaria from *nos>bsk^{RNAi}*; *nos>bsk^{RNAi}, InR^{OE}*; *nos>jra^{RNAi}*; *nos>jra^{RNAi}, InR^{OE}* flies

647   endogenously expressing Myc-GFP co-stained with anti-GFP and anti-1B1. Note that

648   Myc-GFP level in germ cells is markedly lower than that in follicle cells pointed out by

649   arrows.

650   (I) ETC activity in region 2B cysts from ovaries with indicated genotypes. ETC activity is

651   normalized to that of region 2B cysts from the *ctrl* line.

652   Error bars represent SEM. *p < 0.005.
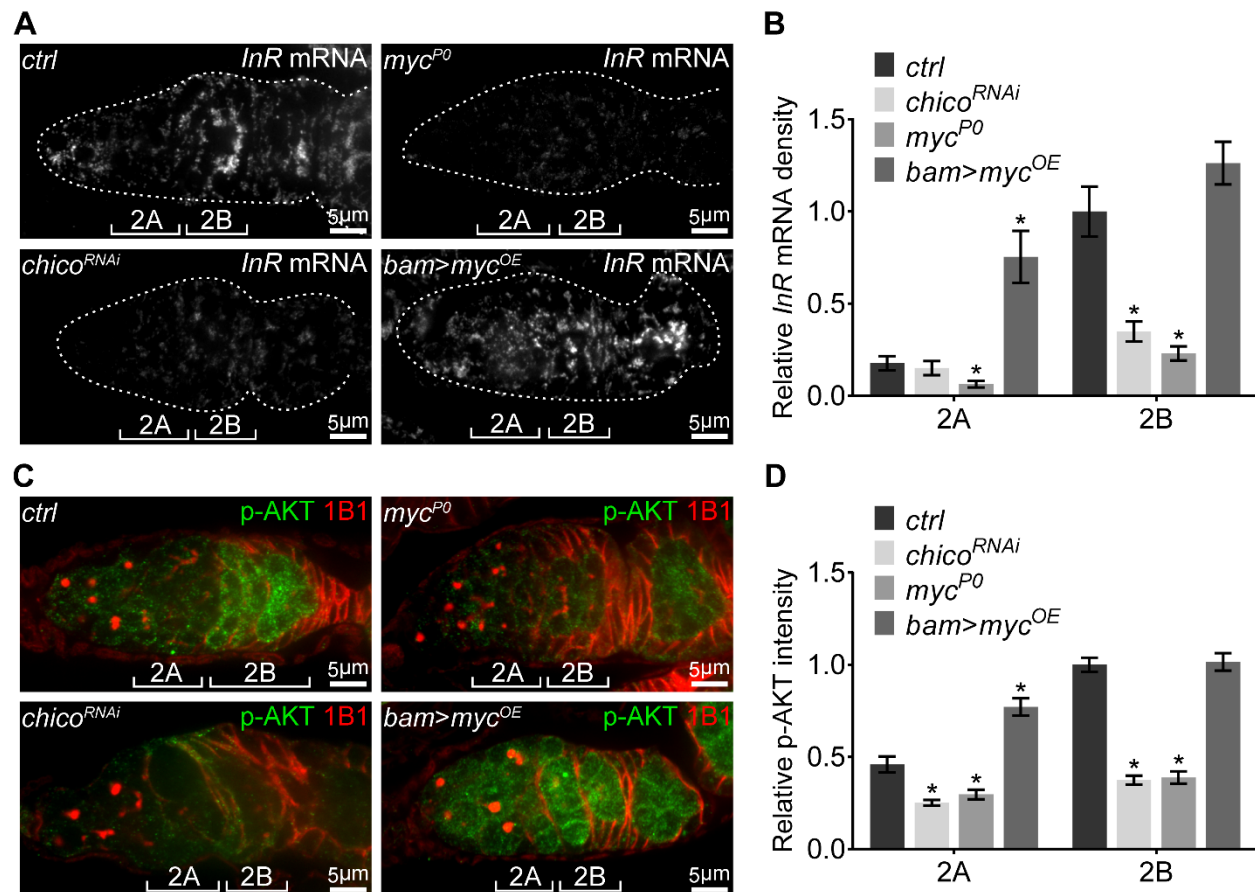
653 **Figure 6**

655 **Figure 6. A positive feedback regulatory loop between IIS and Myc.**

656 (A) Visualization of the *InR* mRNA with fluorescently labelled DNA probes (green) by
657 FISH in germaria from *nos>ctrl*, *nos>chico^{RNAi}*, *myc^{P0}*, and *bam>myc^{OE}* ovaries.
658 Germaria are outlined with dotted lines. Reduction in either IIS or Myc depletes *InR*
659 mRNA in the germarium, while *myc* over-expression in region 2A ectopically induces
660 *InR* mRNA.

661 (B) Quantification of *InR* mRNA intensity from cysts in germarium region 2A and 2B of
662 ovaries with indicated genotypes. Intensities are normalized to the value of *ctrl* at region
663 2B.

664 (C) Germaria from *nos>ctrl*, *nos>chico^{RNAi}*, *myc^{P0}*, and *bam>myc^{OE}* ovaries stained with
665 anti-p-AKT and anti-1B1. Decrease in either IIS or Myc reduces IIS activity in the
666 germarium, while *myc* over-expression in region 2A ectopically induces IIS activity.

667 (D) Quantification of p-AKT intensity in region 2A and 2B cysts of ovaries with indicated
668 genotypes. Intensities are normalized to the value of *ctrl* at region 2B.

669   Error bars represent SEM. *p < 0.005.
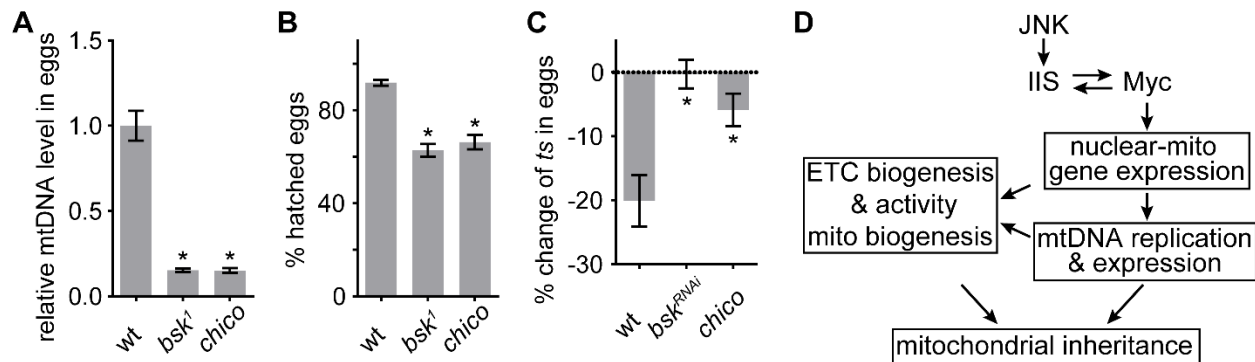
670 **Figure 7**

672 **Figure 7. JNK-IIS relay is essential for mtDNA selective inheritance and fertility.**

673 (A) Quantification of relative mtDNA content in eggs produced by mothers of either GLC

674 for bsk^1 or $chico^{1/KG}$ mutant. Relative mtDNA levels are determined by qPCR for $mt:CoI$

675 and $his4$ copies, and normalized to the level in wt.

676 (B) Hatching rates of eggs produced by female flies of either GLC for bsk^1 or $chico^{1/KG}$

677 mutant are significantly reduced compared to the hatching rates of wt eggs.

678 (C) Quantification of $mt:CoI^{T300I}$ transmission from females with indicated nuclear

679 genotypes. In wt females, the mtDNA mutation is counter-selected, resulting in ~20%

680 fewer mutant mtDNAs in the progeny than in the mothers. This counter-selection is

681 diminished in $chico^{1/KG}$ mutant or $nos>bsk^{RNAi}$ mothers. Mother flies heteroplasmic for

682 $mt:CoI^{T300I}$ were cultured at 29°C.

683 (D) Schematics of the developmental signaling relay initiated from late germarium that

684 primes mitochondrial respiration, and mtDNA replication and inheritance.

685 Error bars represent SEM. *p < 0.005.

686

687

688   **SUPPLEMENTAL INFORMATION**

689

690   **SUPPLEMENTAL TABLES**

691   Table S1 Candidate RNAi screen.

692   Table S2 Differential expression of mRNAs in myc^{P0} mutant ovaries compared with wt

693   ovaries.

694   Table S3 Sequences of FISH probes.

695

696 **SUPPLEMENTAL FIGURES AND FIGURE LEGENDS**
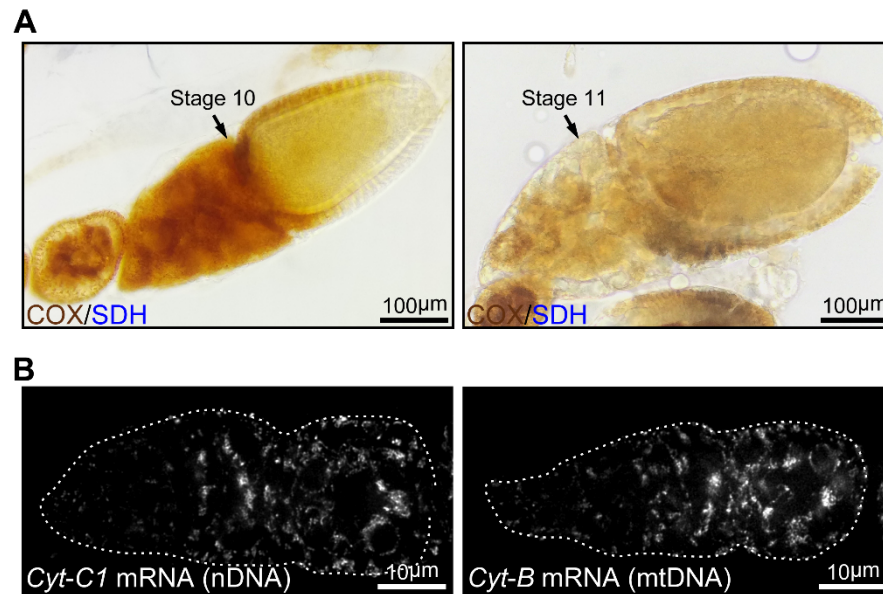
697
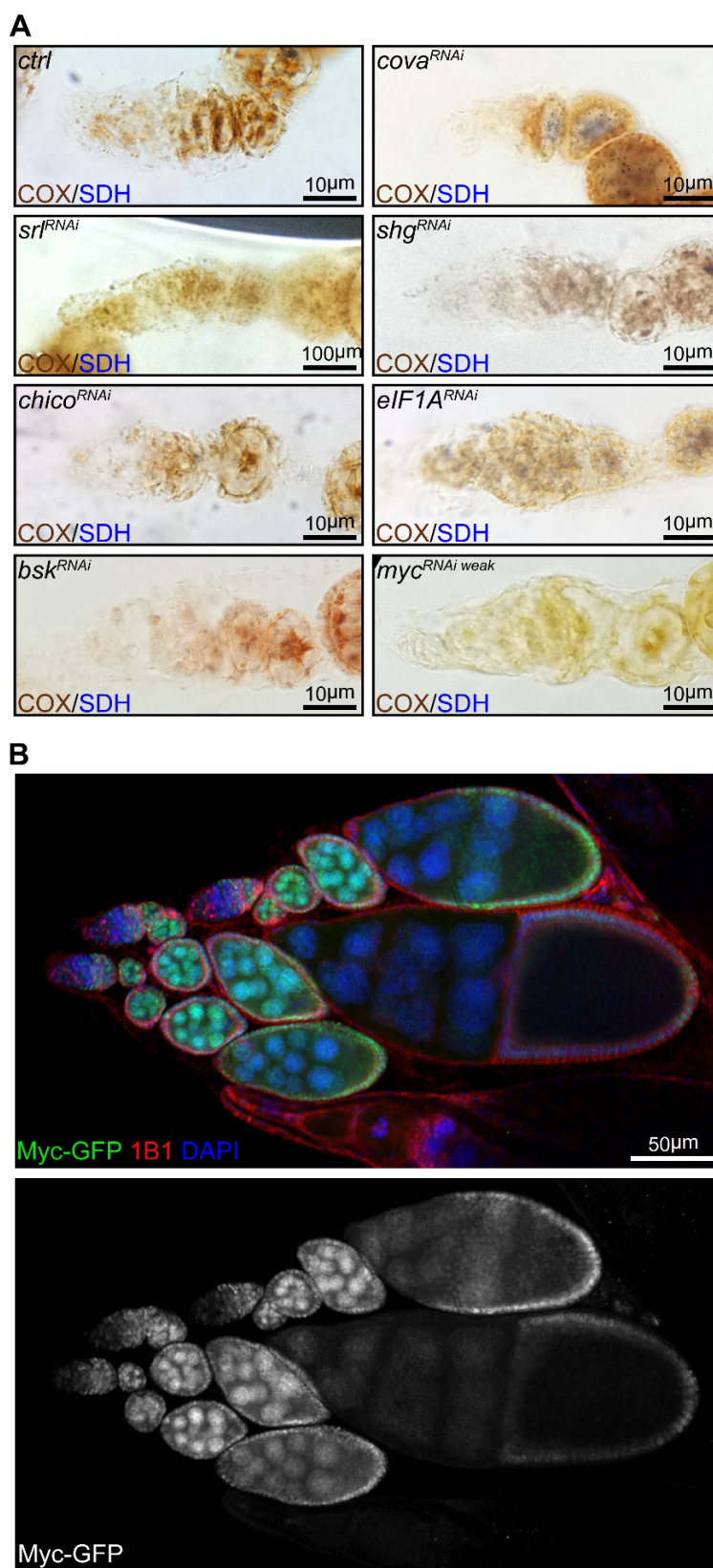
698 **Figure S1**

699

700 **Figure S1. ETC activity at middle stages of oogenesis and expression of complex**

701 **III genes in the germarium. (Related to Figure 1)**

702 (A) Egg chambers from wt flies stained with COX/SDH. Note that ETC activity is high in

703 a stage 10 egg chamber, while it is dramatically reduced in a stage 11 egg chamber.

704 (B) Visualization of the *Cyt-C1* and *Cyt-B* mRNA in germaria from wt flies with

705 fluorescently labelled DNA probes by FISH. Germaria are outlined with dotted lines.

706

Wang et al., 2019

707 **Figure S2**

bioRxiv preprint doi: https://doi.org/10.1101/642314; this version posted May 18, 2019. The copyright holder for this preprint (which was not certified by peer review) is the author/funder, who has granted bioRxiv a license to display the preprint in perpetuity. It is made available under aCC-BY-NC-ND 4.0 International license.

709 **Figure S2. ETC activity in representative candidate RNAi screen and Myc protein**

710 **pattern in the ovary. (Related to Figure 2)**

711 (A) COX/SDH staining for germaria with reduced ETC activity (positive hits) from the

712 candidate RNAi screen.

713 (B) A representative low magnification image of ovarioles from flies endogenously

714 expressing Myc-GFP stained with anti-GFP, anti-1B1, and DAPI. Note that Myc level is

715 low in early germarium stages, becomes high from germarium region 2B, and reduces

716 from the stage 10 egg chamber.

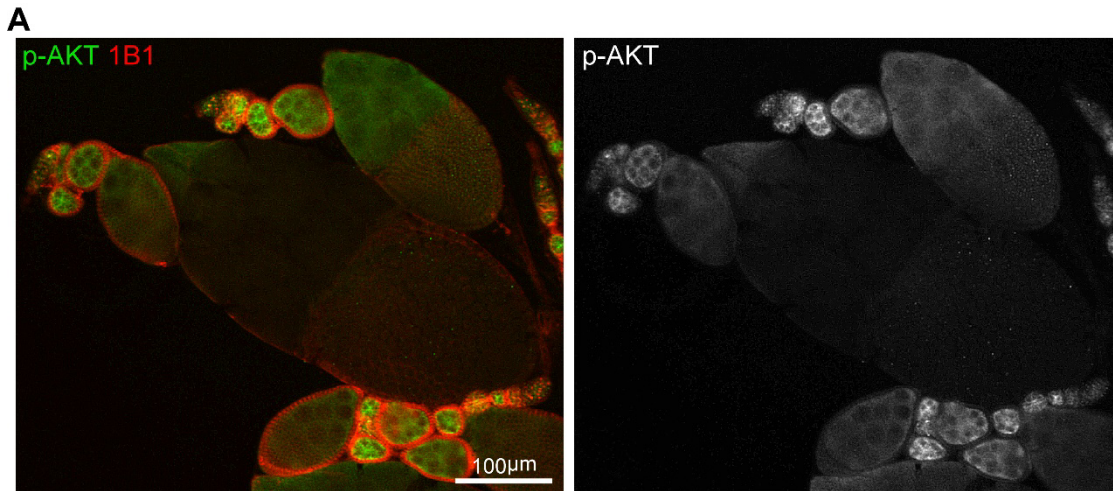717

718 **Figure S3**

A

719

720 **Figure S3. IIS activity in the ovary. (Related to Figure 3)**

721 (A) A low magnification image of ovarioles stained with anti-p-AKT and anti-1B1. Note

722 that IIS activity is low in early germarium stages, becomes high from late germarium,

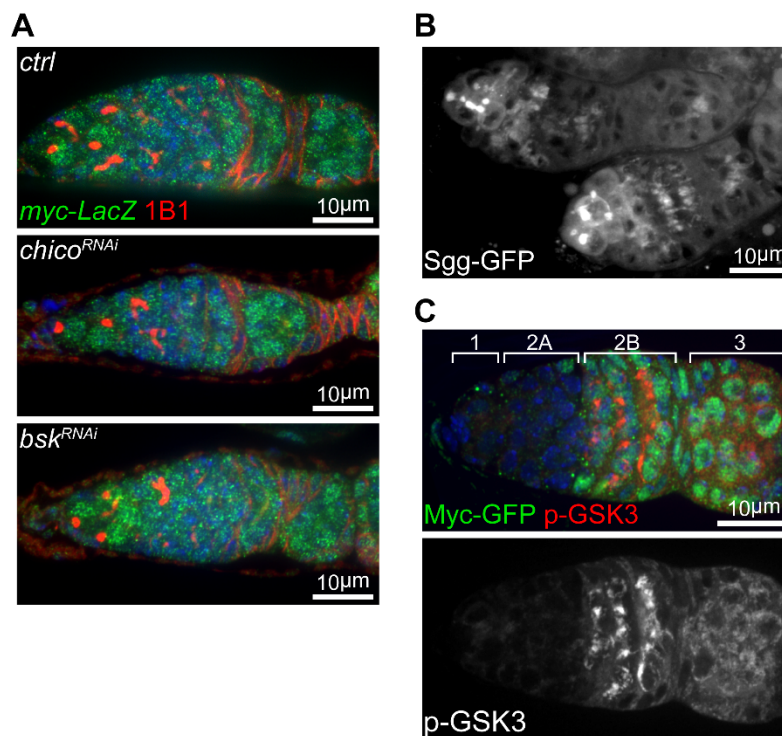723 and decreases from the stage 10 egg chamber, the same pattern as Myc protein.

724

725 **Figure S4**

726

727 **Figure S4. Myc is post-transcriptionally regulated by the IIS-GSK3 cascade.**

728 **(Related to Figure 4)**

729 (A) Germaria from *nos>ctrl*, *nos>chico^RNAi*, and *nos>bsk^RNAi* ovaries expressing LacZ

730 under the control of *myc* endogenous promoter stained with anti-β-galactosidase and

731 anti-1B1.

732 (B) A representative live imaging of germaria from flies expressing GFP-tagged Sgg

733 under its endogenous promoter.

734 (C) A germarium from wt flies endogenously expressing Myc-GFP stained with anti-GFP

735 (green) and anti-p-GSK3 (red). Germarium regions are indicated. Myc protein highly

736 corresponds to inhibited form of GSK3.
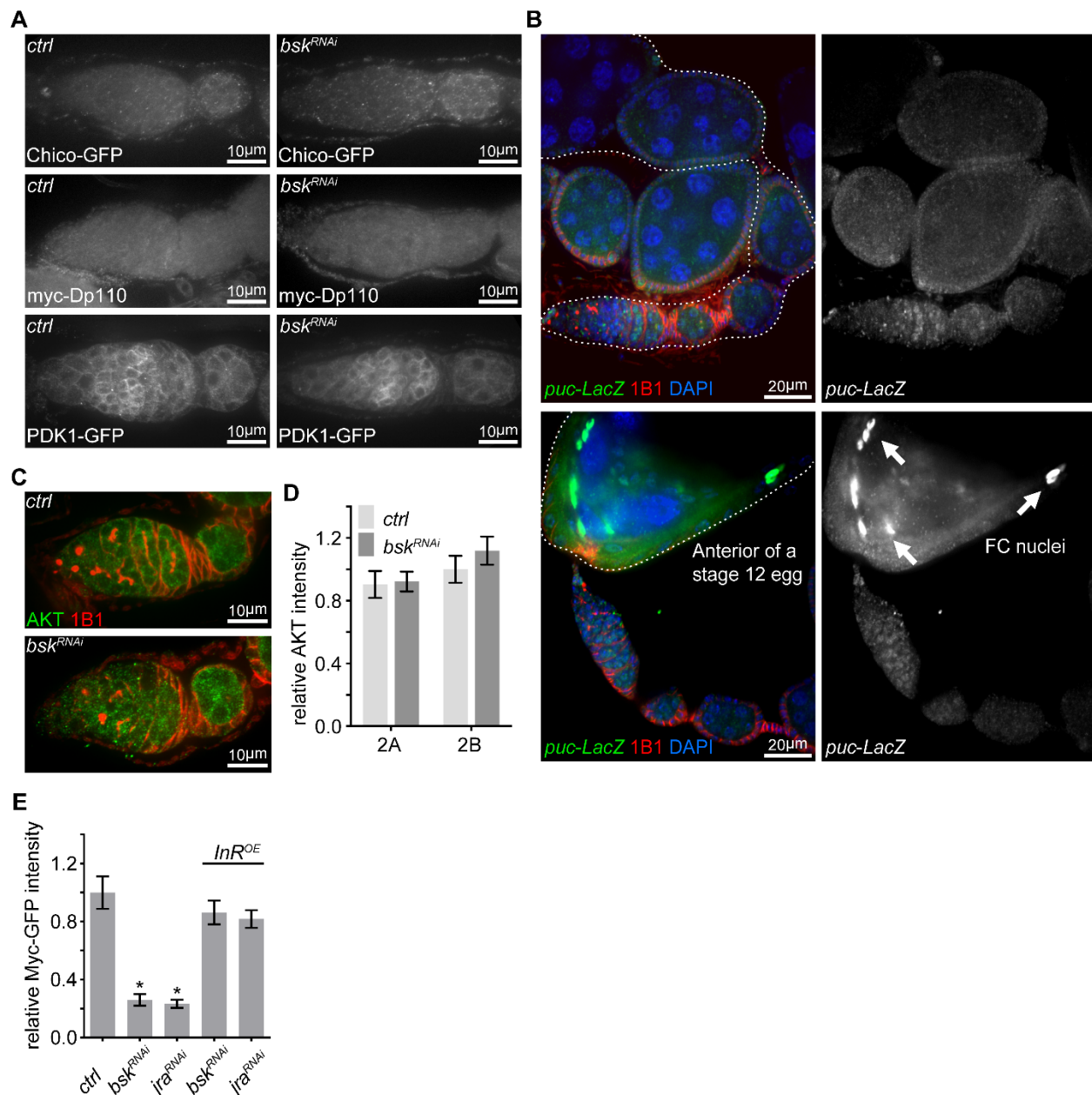
Wang et al., 2019

Fig S5

Fig S5. Other IIS components are not altered by *bsk* RNAi. (Related to Figure 5)

(A) Confocal images for germaria expressing Chico-GFP, myc-Dp110 or PDK1-GFP in the background of *ctrl* or *bsk*[RNAi] from ovaries stained with anti-GFP or anti-myc.

(B) Ovaries expressing LacZ driven by the *puc* promoter stained with anti-β-galactosidase, anti-1B1, and DAPI. Note that JNK activity is moderately induced in late germarium and decreased in the following stages, while JNK activity is much stronger in follicle cells of a maturing egg.

746   (C) Germaria from *nos>ctrl* and *nos>bsk^{RNAi}* flies stained with anti-AKT and anti-1B1.

747   (D) Quantification of AKT intensity from cysts in germarium region 2A and 2B of ovaries

748   with indicated genotypes. Intensities are normalized to the value of *ctrl* at region 2B.

749   (E) Quantification of relative Myc-GFP intensity in region 2B cysts of ovaries illustrated

750   in Fig 5H.

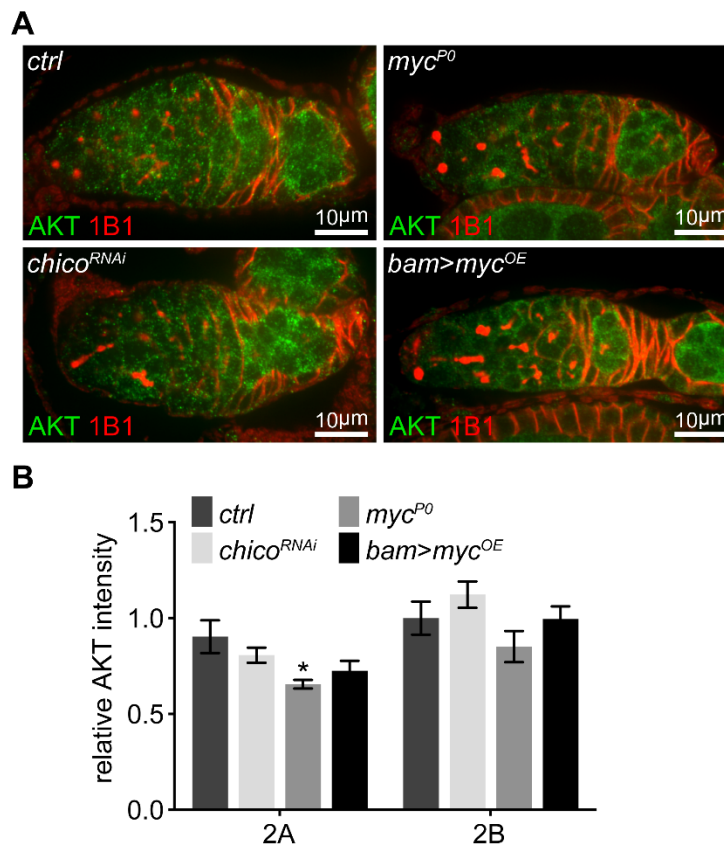751   Error bars represent SEM. *$p < 0.005$.

752   **Figure S6**

753

754   **Figure S6. AKT level is normal when IIS is decreased, but slightly reduced in the**

755   myc^{P0} **mutant. (Related to Figure 6)**

756   (A) Germaria from *nos>ctrl*, *nos>chico^{RNAi}*, *myc^{P0}*, and *bam>myc^{OE}* ovaries stained with

757   anti-AKT and anti-1B1.

758   (B) Quantification of AKT intensity in region 2A and 2B from ovaries with indicated

759   genotypes.

760   Error bars represent SEM. *$p < 0.005$.

761   **STAR☆METHODS**

762   **KEY RESOURCES TABLE**

REAGENT or RESOURCE	SOURCE	IDENTIFIER
Antibodies		
Mouse monoclonal anti-GFP	Roche	11814460001
Mouse monoclonal anti-Hts	Developmental Studies Hybridoma Bank	1B1
Mouse monoclonal anti-ATP5A	ATP5A	ab14748
Rabbit polyclonal anti-GFP	Novus	NB600-308
Rabbit polyclonal anti-dMyc	Santa Cruz Biotechnology	d1-717
Rabbit polyclonal anti-Vasa	Santa Cruz Biotechnology	sc-30210
Rabbit monoclonal anti-p-GSK3	Cell Signaling Technology	9323S
Mouse monoclonal anti-GSK3	Cell Signaling Technology	9832S
Rabbit polyclonal anti-AKT	Cell Signaling Technology	9272S
Rabbit polyclonal anti-p-AKT	Cell Signaling Technology	4054S
Mouse monoclonal β-galactosidase	Promega	Z378A
Chemicals and competent cells		
TMRM	Thermo Fisher Scientific	I34361
MitoTracker™ Green	Thermo Fisher Scientific	M7514
Cytochrome c from equine heart	Sigma-Aldrich	C7752

3,3'-Diaminobenzidine tetrahydrochloride	Sigma-Aldrich	D5905
Catalase from bovine liver	Sigma-Aldrich	C9322
Nitrotetrazolium Blue chloride	Sigma-Aldrich	N6876
Phenazine methosulfate	Sigma-Aldrich	P9625
Sodium succinate	Sigma-Aldrich	S2378
Heparin ammonium salt	Sigma-Aldrich	H6279
Salmon Sperm DNA	Invitrogen	15632011
Critical Commercial Assays		
Click-iT™ Plus EdU Alexa Fluor™ 488 Imaging Kit	Thermo Fisher Scientific	C10637
Ribo-Zero rRNA Removal Kit	Illumina Inc.	MRZH116
Experimental Models: Organisms/Strains		
w^{1118} (wt)	(Zhang et al., 2019)	https://doi.org/10.1016/j.molcel.2019.01.013
ts ($mt:Col^{T300I}\%$)	(Hill et al., 2014)	https://doi.org/10.1038/ng.2920
UAS-Dcr-2; nos-Gal4	Bloomington Drosophila Stock Center	BL25751
nos-Gal4	Bloomington Drosophila Stock Center	BL32563
bam-Gal4	(Chen and McKearin, 2003)	https://doi.org/10.1242/dev.00325
UAS-$LacZ$ ($ctrl$ over-expression)	(Wang et al., 2016)	https://doi.org/10.1093/hmg/ddw067
myc^{P0}	(Johnston et al., 1999)	https://doi.org/10.1016/S0092-8674(00)81512-3

myc-LacZ	Bloomington Drosophila Stock Center	BL12247
puc-LacZ	Bloomington Drosophila Stock Center	BL11173
UAS-myc	(Rhiner et al., 2009)	https://doi.org/10.1242/dev.033340
bsk^1, FRT40A	(Bornstein et al., 2015)	https://doi.org/10.1016/j.neuron.2015.10.023
hs-FLP; ubi-mRFP, FRT40A	(Bornstein et al., 2015)	https://doi.org/10.1016/j.neuron.2015.10.023
thro^{RNAi}	Bloomington Drosophila Stock Center	BL36815
puc^{RNAi}	Bloomington Drosophila Stock Center	BL36085
UAS-InR	Bloomington Drosophila Stock Center	BL8262
chico^1	Bloomington Drosophila Stock Center	BL10738
chico^{KG}	Bloomington Drosophila Stock Center	BL14337
Myc-GFP	Bloomington Drosophila Stock Center	BL38633

Sgg-GFP	Bloomington Drosophila Stock Center	BL66770
Oligonucleotides		
InR chiRNA targeting sequence: CCTTTCCGTAGATGGATGACACC	This paper	
mt:CoI, Xho1 site genotyping F: TGGAGCTATTGGAGGACTAAATCA	(Hill et al., 2014)	https://doi.org/10.1038/ng.2920
mt:CoI, Xho1 site genotyping R: GCTCCTGTTAATGGTCATGGACT	(Hill et al., 2014)	https://doi.org/10.1038/ng.2920
qPCR, *his4*-F: TCCAAGGTATCACGAAGCC	(Zhang et al., 2015)	https://doi.org/10.15252/embr.201439636
qPCR, *his4*-R, Reverse: AACCTTCAGAACGCCAC	(Zhang et al., 2015)	https://doi.org/10.15252/embr.201439636
qPCR, *mt:CoI*-F, Forward: ATTGGAGTTAATTTAACATTTTTTCCTCA	(Zhang et al., 2015)	https://doi.org/10.15252/embr.201439636
qPCR, *mt:CoI*-R, Reverse: AGTTGATACAATATTTCATGTTGTGTAAG	(Zhang et al., 2015)	https://doi.org/10.15252/embr.201439636
Software and Algorithms		
ImageJ	NIH	https://imagej.nih.gov/ij/
GraphPad Prism7	GraphPad Software, Inc.	http://www.graphpad.com/

763

764 **CONTACT FOR REAGENT AND RESOURCE SHARING**

765 Further information and requests for resources and reagents should be directed

766 to and will be fulfilled by the Lead Contact, Hong Xu (Hong.Xu@nih.gov).

767

768 **EXPERIMENTAL MODEL AND SUBJECT DETAILS**

Drosophila Genetics

Flies were maintained on standard BDSC cornmeal medium at 25°C. RNAi lines obtained from either the Bloomington Stock Center or the Vienna Drosophila RNAi Center are listed in KEY RESOURCES TABLE. Embryo hatch assay was performed as previously described (Zhang et al., 2019).

METHOD DETAILS

Measurement of mtDNA copy number and quantification of heteroplasmy

Total DNA was isolated from eggs with QIAamp DNA Micro Kit (Qiagen). The mtDNA copy number was measured by quantitative real-time PCR with primers targeting to cytochrome c oxidase subunit I (mt:CoI) and His4 genes. Quantification of heteroplasmy was performed as described previously (Zhang et al., 2019). Heteroplasmic female flies were transferred from 18 °C to 29 °C after eclosion. Each female was mated with 5 wt males. Ten eggs produced from the day 7 at 29 °C were collected. The genomic DNA from female flies and eggs was extracted and their heteroplasmy levels were determined as shown before (Hill et al., 2014).

CRISPR/Cas9 in flies

To tag InR with EGFP into its endogenous locus, a DNA fragment comprising 1kb upstream of *InR* stop codon, EGFP, a fragment containing GMR-Hid flanked by FRT sequences, and 1kb downstream of *InR* stop codon was inserted into a pOT2 vector. This donor construct and a chiRNA construct inserted with a targeting sequence CCTTTCCGTAGATGGATGACACC were injected into the embryos of M{vas-Cas9}ZH-2A (BL51323) by Bestgene Inc.. G1 adults were screened for loss of eye phenotype. Insertion events were further confirmed by PCR using two pairs of primers: 1, InR-GenomeF1: ATGATGTCATCGGTGGGTCCTCAC, EGFP-seqR: CTTGTAGTTGCCGTCGTCCTTGAA; 2, InR-GenomeF2: AGCACATTGTGTCAGTCTTCG, InR-GenomeR: CTCATTTTCCGAAGCTTGGCTTCC.

RNA sequencing and RNA-seq analysis

Total RNA was extracted by Trizol (Life Technologies) following its standard protocol. Poly (A) capture libraries were generated at the DNA Sequencing and Genomics Core, NHLBI, NIH. RNA sequencing was performed with using an Hiseq3000

800   (Illumina) and 75-bp pair-end reads were generated at the DNA Sequencing and

801   Genomics Core, NHLBI, NIH. Raw sequence reads were quality-trimmed using Trim

802   Galore! (v0.3.7) and aligned using Tophat2 (v2.0.14) against the Dm6 reference

803   genome. Uniquely mapped paired-end reads were then used for subsequent analyses.

804   FeatureCounts was used for gene level abundance estimation. Principal component

805   analysis (PCA) was used to assess outlier samples. Genes were kept in the analysis if

806   they had Counts Per Million (CPM>1) in at least half the samples. We adjusted for

807   multiple testing by reporting the FDR q-values for each feature. Features with q < 5%

808   were declared as genome-wide significant. Genes with 3 or more fold changes on

809   mRNA level in myc^{P0} mutant compared with wt were considered differentially

810   expressed. Gene Ontology (GO) was used to analyze gene set enrichment. FDR q-

811   values were estimated to correct the p-values for the multiple testing issue.

812   **Live image**

813   Live image of fly ovaries was performed as previously reported (Zhang et al.,

814   2019). Ovaries from wt flies were stained with TMRM and MTgreen for 20 min followed

815   by PBS washes for 3 times. Ovaries from Sgg-GFP flies were dissected. Ovarioles were

816   isolated and immerged in halocarbon oil on coverslips, then live imaged with a Perkin

817   Elmer Ultraview system. The ratiometric image was generated with ImageJ, which the

818   intensity of red channel is divided by that of green channel.

819   **Immunohistochemistry and fluorescence RNA in situ hybridization (FISH)**

820   Ovary dissection, immunostaining and EdU incorporation were performed as

821   described before (Hill et al., 2014). Stellaris FISH probes against, *Cyt-C1*, *Cyt-B*, *CoxIV*,

822   *CoxIII*, or *InR* mRNA were synthesized from Bioserch Technologies. Sequences of the

823   probes are shown in table S3. FISH of *Drosophila* ovaries was conducted as previously

824   described (Trcek et al., 2017). Confocal images were collected by a Perkin Elmer

825   Ultraview system or Instant Sim (iSIM) Super-Resolution Microscope. All images were

826   processed with Image J.

827

828   **QUANTIFICATION AND STATISTICAL ANALYSIS**

829   All statistical analyses were conducted with Prism 7 (GraphPad Software). Error
830   bars in all charts represent standard errors. P values were performed with Two-tailed
831   Student's t test. Statistical significance of difference was considered when $P < 0.05$.

832

833   **DATA AVAILABILITY**

834   The data were deposited in Gene Expression Omnibus of NCBI (Edgar et al.,
835   2002) and will be available with accession number (GEO: GSE126997).

836

837   **SUPPLEMENTAL REFERENCE**

838   Bornstein, B., Zahavi, E.E., Gelley, S., Zoosman, M., Yaniv, S.P., Fuchs, O., Porat, Z.,
839   Perlson, E., and Schuldiner, O. (2015). Developmental Axon Pruning Requires
840   Destabilization of Cell Adhesion by JNK Signaling. Neuron *88*, 926-940.

841   Chen, D., and McKearin, D.M. (2003). A discrete transcriptional silencer in the bam
842   gene determines asymmetric division of the Drosophila germline stem cell.
843   Development *130*, 1159-1170.

844   Edgar, R., Domrachev, M., and Lash, A.E. (2002). Gene Expression Omnibus: NCBI
845   gene expression and hybridization array data repository. Nucleic Acids Res *30*, 207-
846   210.

847   Hill, J.H., Chen, Z., and Xu, H. (2014). Selective propagation of functional mitochondrial
848   DNA during oogenesis restricts the transmission of a deleterious mitochondrial variant.
849   Nat Genet *46*, 389-392.

850   Johnston, L.A., Prober, D.A., Edgar, B.A., Eisenman, R.N., and Gallant, P. (1999).
851   Drosophila myc regulates cellular growth during development. Cell *98*, 779-790.

852   Rhiner, C., Diaz, B., Portela, M., Poyatos, J.F., Fernandez-Ruiz, I., Lopez-Gay, J.M.,
853   Gerlitz, O., and Moreno, E. (2009). Persistent competition among stem cells and their
854   daughters in the Drosophila ovary germline niche. Development *136*, 995-1006.

855   Trcek, T., Lionnet, T., Shroff, H., and Lehmann, R. (2017). mRNA quantification using
856   single-molecule FISH in Drosophila embryos. Nat Protoc *12*, 1326-1348.

857   Wang, Z.H., Clark, C., and Geisbrecht, E.R. (2016). Drosophila clueless is involved in
858   Parkin-dependent mitophagy by promoting VCP-mediated Marf degradation. Hum Mol
859   Genet *25*, 1946-1964.

860   Zhang, F., Qi, Y., Zhou, K., Zhang, G., Linask, K., and Xu, H. (2015). The cAMP
861   phosphodiesterase Prune localizes to the mitochondrial matrix and promotes mtDNA
862   replication by stabilizing TFAM. EMBO Rep *16*, 520-527.
863   Zhang, Y., Wang, Z.H., Liu, Y., Chen, Y., Sun, N., Gucek, M., Zhang, F., and Xu, H.
864   (2019). PINK1 Inhibits Local Protein Synthesis to Limit Transmission of Deleterious
865   Mitochondrial DNA Mutations. Mol Cell *73*, 1127-1137 e1125.

866

867

868

869

870